Robotic Sorting of Zebrafish Embryos

Alioune Diouf, Ferhat Sadak, Edison Gerena, Abdelkrim Mannioui, Daniela Zizioli, Irene Fassi, Mokrane Boudaoud, Giovanni Legnani, Sinan Haliyo

Robotic Sorting of Zebrafish Embryos

Alioune Diouf[1,2*], Ferhat Sadak[1,3†], Edison Gerena[1†], Irene Fassi[4†], Mokrane Boudaoud[1†], Giovanni Legnani[2†], Sinan Haliyo[1†]

[1*]Sorbonne Université, , Institut des Systèmes Intelligents et de Robotique (ISIR) , Paris, France.
[2]Department of Industrial Engineering, Universita degli Studi di Brescia, Brescia, Italy.
[3]Department of Mechanical Engineering, Bartin University, Bartin, Türkiye.
[4] Institute of Intelligent Industrial Technologies and Systems for Advanced Manufacturing National Research Council of Italy, Milan,Italy.

*Corresponding author(s). E-mail(s): diouf@isir.upmc.com;
Contributing authors: fsadak@bartin.edu.tr; edison.gerena@isir.upmc.fr;
irene.Fassi@stiima.cnr.it; mokrane.boudaoud@isir.upmc.fr ;
giovanni.legnani@unibs.it ; sinan.haliyo@isir.upmc.fr ;
†These authors contributed equally to this work.

Abstract

Transcriptomics and metabolomics, two biological research fields that need large numbers of zebrafish embryos, require the removal of unfertilized or nonviable zebrafish embryos. Biologists routinely conduct the tedious, error-prone, and time-consuming manual sorting of embryos. We suggest a novel approach that combines deep learning and microfluidics for automated sorting to overcome this difficulty. To determine the developmental stage and viability of zebrafish eggs, we trained an optimized YOLOv5 model with 95% accuracy and a processing speed of 10.6 ms per frame, classifying them as dead, unfertilized, or alive. The eggs are contained in traps on a microfluidic chip using micro-pumps. After that, the deep learning system can identify and automatically sort the eggs according to their viability by positioning this chip on an XYZ motorized stage.The sorting experiment was conducted in two modes: without feedback and with feedback while using the dead egg position. The first one had a sorting success rate of 90% as opposed to 97.9% for the feedback mode with 3 seconds required for each dead egg. This automated approach provides a precise and efficient way to handle a large number of zebrafish embryos while also greatly reducing the workload

associated with manual sorting. The success rates attained demonstrate the usefulness and effectiveness of our suggested methodology, opening new avenues for biological research involving accurate embryo selection.

Keywords: Zebrafish embryo, Deep Learning, Micro robotics, Microfluidic, YOLOv5

1 Introduction

Research often utilizes patients cells or tissue samples, but to determine if a mutation in a specific gene can cause a patient's symptoms, experimental animal models are often needed. The zebrafish (danio rerio) has emerged as an important model organism for developmental genetic studies as well as for drug discovery. Researches based on the zebrafish have brought to new advances in numerous medical fields. Its analysis is crucial in the study of hematopoietic, cardiovascular and vascular disorders, as well as of tumours, neurodegenerative and neuromuscular diseases like Alzheimer's syndrome, Huntington's disease and Duchenne muscular dystrophy. These Zebrafish mutants are therefore used to simulate the human pathologies in order to study effective pharmacological therapies. However, manual handling of zebrafish embryos is a tedious and time-consuming task due to their small size and the large quantity of samples usually required in an experimental setup [1]. The need for a fast and automated screening method to improve working conditions with zebrafish embryos and larvae has become critical. Retrieving and sorting eggs after a spawning event and removing the unfertilized or dead ones is of high importance for maintaining optimal growth conditions and promoting the well-being of growing embryos. Contaminated hatching water stimulate bacterial proliferation among the eggs which secrete enzymes to degrade the egg shells, leading to premature hatching and death. Similarly, fungi spores can develop and spread over dead eggs and eventually spread to healthy eggs, compromising embryos development. Therefore, removing unfertilized eggs or dead embryos is crucial to prevent batch contamination as spoiled eggs can serve as a growth medium to deadly microorganisms [2]. Including unfertilized eggs or premature dead embryos in a cohort of tested embryos can lead to non-precise results as unfertilized eggs will increase the death rate following a screening assay. Therefore, early sorting of embryos should be performed not only to prevent batch contamination but also to exclude any irrelevant samples from the experiment [3].

The current state of technology for automated microscopic imaging of zebrafish and interpreting these images is well-established. Nevertheless, automating the sample preparation process offers further opportunity for unique developments [4]. To assess the trend in the cell preparation domain, powerful strategies to sort cells utilizing high spatial and often time-resolved data have emerged, collectively called Image-Based Cell Sorting (IBCS) [5]. These IBCS platforms address major limitations of commonly used technologies, such as Fluorescence-Activated Cell Sorting (FACS) and Magnetic Activated Cell Sorting (MACS) which are the most commercialized methods for sorting cells. The Big Data Era and the development of Deep Learning (DL), image detection will become the mainstream for single cell analysis [5]. DL techniques enhance the

detection procedure compared to conventional techniques as it reduces the expensive computational time as well as detecting irregular shapes which is common among the biological cells [6]. Researchers have developed a classification software using SVM able to differentiate wild-type embryos from mutant individuals with an accuracy of 79-99% depending on the test and system [7]. A sorting system based on Convolutional Neural Networks (CNN) is capable of sorting and placing individual zebrafish eggs in multiwell plates [8]. A fully automated pipetting sorting system based on template-matching algorithms made it possible to classify zebrafish eggs and sort them with a robot [9]. Although several machine learning approaches are available and can achieve reliable detection results but Deep Neural Networks (DNN) is the most popular system exploited so far for zebrafish egg detection [6, 10, 11]. EmbryoNet is a software based on a DNN model to identify zebrafish embryo signaling mutants in an unbiased manner [12]. A system based on Inception v3 allows to detect and performs microinjection on zebrafish eggs [13].A machine vision guided robot based on YOLOv4 is developed for fully automated embryonic detection and microinjection [14].

Microfluidics-based approaches are in their early stages and hold significant importance. The fabrication of microfluidic chips becomes economically viable once their design is established, potentially reducing the price barrier for widespread adoption. As an investigative tool, LOC (Lab-On-Chip) represents a new direction that may miniaturize and revolutionize research in toxicity and physiology in vivo [15]. Compared to other non-contact methods for manipulating cells, microfluidics is interesting as it can accommodate different actuation techniques, in addition to flow-control based approaches [16]. However, in case of using external activation, electric or optic, there is currently no guarantee that the field will not damage or badly influence the targeted cell. Using only the fluid's power on the cells guaranteed the cells to stay in liquid medium all the process. Also, with the possibility of designing microfluidic chips, cell immobilization chambers can then be created. Combining microfluidic approaches with DL to automate sorting and selection of zebrafish embryos might replace sample manipulation steps that researchers currently perform manually [4]. Microfluidic chip has been used with zebrafish embryos but more for culture, perfusion systems [17, 18]. This work describes a zebrafish egg sorting system based on robotic, microfluidic and DL. While zebrafish egg classification systems have been well-established in the literature, fast and precise zebrafish egg sorting systems have not received much attention and exploration.

2 Materials and methods

2.1 System overview

A DL model for zebrafish permit to sort dead or unfertilized embryos and viable embryos of stage 1 or other stage of development. The process is conducted in two phases: the phase of filling the traps of the microfluidic chip with zebrafish embryos then the robotic sorting phase.

2.1.1 Filling process

This is the phase where zebrafish embryos measuring approximately 1mm are placed in cavites. The idea of placement is to facilitate and organize sorting later.

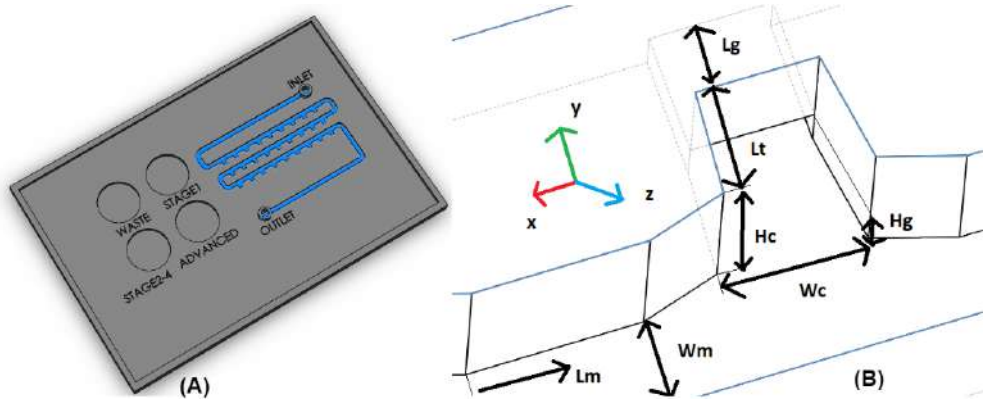

Fig. 1 (A): Microfluidic chip design. (B): The geometric parameters of a single cavity.

During the filling phase, the eggs swim in the water injected into the channel of the microfluidic chip and fall into designed traps (see Fig.2(B)). A single egg can fill a trap and the others slide over it to pass through the other traps. This method is based on gravity and sliding of embryos in traps which has shown its effectiveness for immobilization in many previous works with zebrafish embryos. The trapping of zebrafish embryos in microfluidic devices relies on the forces generated by fluid flow within the microchannel. These forces are essential for directing the embryos towards a trapping cavity where they can be held in place. The transport passageway facilitates the flow of fluid, which carries a component force directed towards the trapping cavity, effectively trapping the embryo. The magnitude of this component force is closely related to the geometric parameters of the trapping cavity. Figure 1(B) illustrates these geometric parameters and their association with the size of the trapping component. These parameters may include dimensions such as width, length, and depth of the trapping cavity, among others. Tang et al. [19] describe that the ability to trap embryos depends on the flow resistance along two pathways:

- Path 1 (Rx): Flow resistance along the main channel.
- Path 2 (Ry): Flow resistance along the trapping cavity direction

According to the work [20], the flow resistance along the main channel (Path 1) and along the trapping cavity direction (Path 2), can be described as :

$$\frac{R_x}{R_y} = \left[\frac{w_c^4}{H_c L_t \left(W_c + H_c\right)^2} + \frac{w_c^4}{H_g L_g \left(W_c + H_g\right)^2} \right] . \frac{H_c L_m \left(W_m + H_c\right)^2}{W_m^4} \tag{1}$$

where $W_{(.)}$ is the width of the channel, $H_{(.)}$ is height, and the $L_{(.)}$ is the length. Letter m , c , and t stand for the main channel, trapping cavities, and transport passageway (behand the cavities) separately. Embryos can be effectively trapped when the flow resistance along both the main channel and the trapping cavity direction are appropriately balanced. This balance ensures that the fluid flow exerts a sufficient force to direct the embryos towards and eventually trap them within the designated cavity. Adjusting the geometric parameters of the trapping cavity can influence this balance and hence affect the trapping efficiency of zebrafish embryos in microfluidic systems. To ensure that the trapping cavity can provide enough force to the embryo during the trapping process, it's necessary to adjust the cavity-related parameters (H_g, W_c, L_g, L_t) in such a way that the flow resistance ratio $Rx : Ry$ is greater than 1. This ensures that the flow resistance along the main channel (Rx) is higher than the flow resistance along the trapping cavity direction (Ry), allowing for effective trapping of embryos. The detailed parameters of the channel should be adjusted according to equation 1 to achieve the desired trapping and release behaviors of the embryos. The specific values for these parameters found for this study are in Table 1.

Table 1 The parameters of the channel

Parameters	Size/mm
Lm	20
Wm	3
Lg	1
Lt	1.5
Hc	1.5
Wc	1.5
Hg	0.5

2.1.2 Robotic Sorting process

Once eggs are immobilized in traps on the microfluidic chip , the cover is removed and the chip is placed on a motorized XYZ-stage (see Fig.3). The stage placed above a DL system moves the microfluidic chip such as each trap will be examined. The cell classification algorithm will be used to decide to remove or to keep the concerned egg. A micromanipulator with a glass pipette as an effector is used to suck and hold the concerned egg to finally place it in the waste part of the chip (see Fig.4). The automated suction process involves the utilization of a piezoelectric water pump that is connected to the holding pipette. This pump is activated once the holding pipette reaches the designated pick-up point. *Google Colab's Tesla T4* GPU was used for DL model training. Figure 11 shows the different devices for sorting process. The experiment was carried out with the uMp manipulator from *Sensapex*, the XYZ-stage LNR50D and DRV250 stepper motors from *Thorlabs*. The vision system comprises a UI-3590CP-C-HQ R2 USB camera from *IDS Imaging Development Systems*, a LM50HC-VIS-SW

lens from *Kowa* and OZB-A4515 6W LED lights from *Kern Optics*. *Bartels mikrotechnik's* piezoelectrip mp6-liq micropumps were used for cell suction as well as for the zebrafish embryo filling system in the traps of the microfluidic chip.

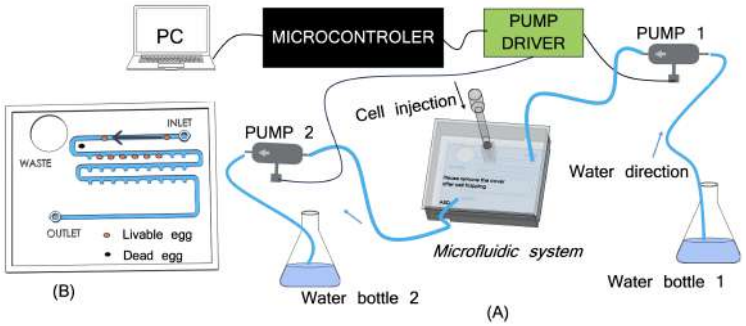

Fig. 2 PHASE 1 : (A): Overview of the filling system, egg are injected with the pipette from the top , (B) : Close look-up to the chip when eggs are injected

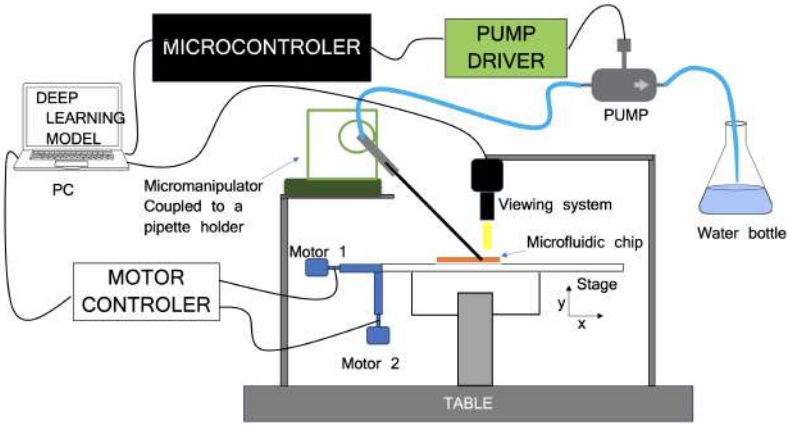

Fig. 3 PHASE 2 : Schematic overview of the sorting system.

2.2 Chip Design and Fabrication

The microfluidic chip comprises an inlet and an outlet, along with traps designated for cell placement. A waste part is where dead eggs are placed by the micromanipulator (see Fig.1). The other parts will be filled by cells at the corresponding stage of developmentThe chip is designed with the 3D CAD software : *Solidworks 2021* and printed using *Formlab's Form 3+* printer with clear V4 resin. After printing the chip is cleaned with isopropanol then placed in UV light for 30 min at 60°C. A cover where also eggs can be injected made with the same resin is placed above the chip durin the filling process.

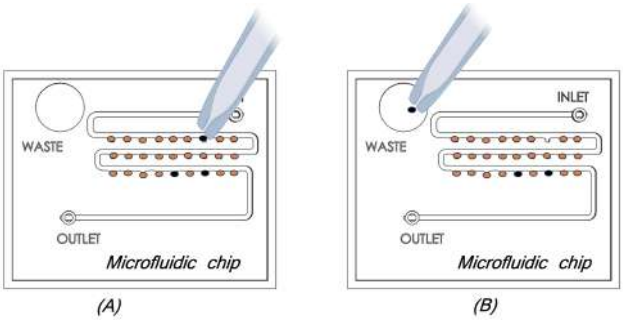

Fig. 4 Pick and place process: (A) Dead or unfertilized embryo being picked. (B) : placed on waste part. Dead cell are black dots and orange are for livable.

2.3 Data collection, labelling and augmentation

The dataset collection was conducted during the first 5 hours after the immediate collection of fresh zebrafish embryos. The zebrafish embryo images were captured at different developmental stages. Images were collected using a combination of an external USB camera UI-3590CP-C-HQ R2 from the manufacturer *IDS Imaging Development Systems* connected to the microscope *Nikon* SMZ800N. So, 1061 images were taken and for the purpose of dataset preparations, the online tool called *RoboFlow* was used. Images are labelled into seven classes : $'stage1'$, $'stage2-4'$, $'advanced'$, $'dead'$, $'returned'$, $'empty'$, $'holder'$.

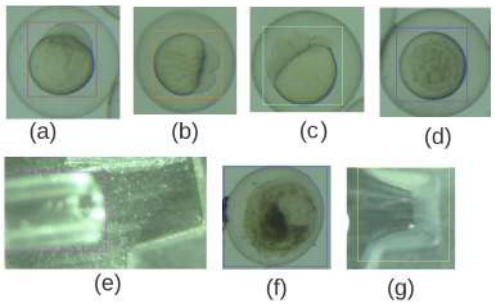

Fig. 5 Differents classes of the model. (a) : $stage1$, (b) : $stage2-4$, (c) : $advanced$, (d) : $returned$, (e) : $holder$, (f) : $dead$. (g) : $empty$

Especially since many study with zebrafish are generally done at the primary stage like microinjection, it is then necessary to detect and differentiate stages 1 and 2 or 4. So after 1 hour post fertilization (hpf), if an egg remains at stage 1, it means that it is unfertilized. Advanced stages, ie above stage 4, are combined in a single class. the $'empty'$ class represents an empty cavity and the $'holder'$ class represents the tip of the pipette which will suck up the embryos Augmented data is driven from original data with some minor changes. In the case of image augmentation, geometric and color space transformations are made (flipping, resizing, cropping, brightness, contrast) to

increase the size and diversity of the training set. Rotation, brightness and saturation operations was performed. Image augmentation techniques like random rotation are commonly used in computer vision tasks to augment the training dataset, thereby increasing its diversity and reducing overfitting. Random rotation introduces variability into the training data, which enables the model to learn to recognize objects or patterns from different perspectives, making it more resilient to variations in real-world scenarios where the camera angle may vary. The eggs swim in the water which means that they rotate arbitrarily by the action of the flow, so applying a rotation augmentation is suitable for a more powerful model. Applying a brightness augmentation makes sense because the model may be used in scenarios where the brightness varies. For example the brightness varies from different microscope images. Adjusting the saturation of images during training make it possible to simulate different color environments and conditions, allowing the model to learn features that are invariant to changes in color saturation. This can help the model generalize better to real-world scenarios where the colors may vary significantly. These operations resulted in a more

Table 2 Data augmentation parameters

Operation	Values
Rotation	-15° and 15°
Brightness	-25% and 25%
Saturation	-25% and 25%

larger, augmented training dataset with 2302 images.

2.4 Description and evaluation of YOLOv5 algorithm

A recent version of the YOLO (*You Only Look Once*) algorithm: YOLOv5 [21] was employed. YOLOv5 builds upon the previous versions, incorporating various improvements in terms of speed, accuracy, and efficiency.Its architecture is composed :

- Backbone: YOLOv5 uses a CSPDarknet53 backbone as its feature extractor. CSPDarknet53 is a variant of Darknet, which is a deep neural network architecture designed for object detection tasks. CSPDarknet53 includes a "cross-stage partial" (CSP) connection scheme, which enhances feature reuse and gradient flow, leading to improved performance.
- Neck: A novel neck architecture called PANet (Path Aggregation Network) is introduced. PANet is designed to aggregate features at different scales and resolutions efficiently, enabling the model to detect objects of varying sizes effectively.
- Head: The detection head of YOLOv5 consists of several convolutional layers responsible for predicting bounding boxes and object classes. YOLOv5 predicts bounding boxes using anchor boxes and employs a variant of the focal loss function to handle class imbalance during training.

Overall, YOLOv5 is designed to provide a good balance between speed and accuracy, making it suitable for various real-time object detection applications, including autonomous vehicles, surveillance systems, and robotics. Its modular architecture and different variants offer flexibility to accommodate different computational constraints and application requirements. YOLOv5's speed is an important criterion in the sorting system because zebrafish embryo sorting must be done quickly, especially at the first stage of development in order to be able to carry out biological studies like microinjection before they move on to the later stages of development. The YOLOv5 training process involves optimizing several loss functions to ensure accurate object detection. The loss function is the combination of loss functions for the bounding box, classification, and confidence. Equation 2 represents the overall loss function of YOLOv5 :

$$loss_{YOLOv5} = loss_{bbox} + loss_{class} + loss_{conf} \tag{2}$$

Where *conf* refers to confidence, *bbox* to bounding box and *class* to classification. The box loss measures how well the predicted bounding box covers the object and accurately locates its center. It evaluates the spatial accuracy of the predicted bounding boxes. Objectness measures the likelihood that an object is present within a specific region of interest. It helps in distinguishing between true objects and background clutter. The classification loss evaluates how accurately the model predicts the correct class label for the detected object. It assesses the algorithm's ability to classify objects into predefined categories. Common evaluation metrics for DL are precision (P), which is precision rate, recall rate (R) and mean average precision (mAP) and Intersection over Union (IoU) . The expressions are as follows:

$$P = \frac{TP}{(TP + FP)} \tag{3}$$

$$R = \frac{TP}{(TP + FN)} \tag{4}$$

$$IoU = \frac{Area\,of\,Overlap}{Area\,of\,Union} \tag{5}$$

IoU is a measure of how well the predicted bounding box overlaps with the ground-truth bounding box as shown in Equation 5. Among them, true positives (TP), false positives (FP), and false negatives (FN), represent positive samples with correct classification, negative samples with incorrect classification, and positive samples with incorrect classification, respectively. AP is the average accuracy rate, which is the integral of the P index to the R index; mAP is the average accuracy of the mean, which means that the AP value of each category is summed, and then divided by all

categories, i.e., the average value. It is defined as follows:

$$mAP = \frac{1}{|Q_R|} \sum_{q=Q_R} AP(q) \tag{6}$$

A high mAP means that the model has both a low false negative and a low false positive rate. The higher the mAP, the more precise and the higher the recall is for the model. Additionally, $mAP@0.5$ and $mAP@0.5:0.95$, which assess the mAP over different IoU thresholds from 0.5 to 0.95.

2.5 Optimization of the hyperparameters

Hyperparameter tuning in object detection involves selecting the best values for parameters that shape the model's architecture and training process. These parameters significantly affect the model's accuracy, precision, and recall. The process of hyperparameter tuning entails systematically testing different combinations of these parameters to identify the configuration that maximizes the chosen performance metric, like accuracy or mAP. Common techniques for hyperparameter tuning include grid search, random search, Bayesian optimization, and genetic algorithms. Each method aims to efficiently explore the hyperparameter space to find the optimal configuration for the object detection model. Selecting the optimal hyperparameters for YOLOv5 is particularly challenging due to the vast parameter space involved. Initially, we utilized the hyperparameters provided by the official YOLOv5 model as a starting point and fine-tuned them for our custom dataset. Each model underwent training and evaluation using an objective function, where we employed mAP metrics with a specific weighting scheme to ensure consistency with our evaluation method. Models were selected based on a fitness score derived from the evaluation metrics, aiming to maximize this score. These models were then subjected to a genetic algorithm mutation operator, which introduced random perturbations to explore new configurations while preserving successful solutions. The iterations continued for 10 generations. The final hyperparameters were chosen based on the YOLOv5 model with the highest evaluation metric score at the end of the iterations. We successfully tuned all 29 hyperparameters for YOLOv5, demonstrating its effectiveness in improving overall detection accuracy. Figure 8 illustrates the hyperparameter tuning process using a Genetic Algorithm, with the fitness score plotted on the y-axis and hyperparameter values on the x-axis, where greater concentrations are highlighted in yellow.

3 Results and discussion

The training was completed in 100 epochs, a batch size of 16 using YOLOv5x which is the extra large version of YOLOv5. This version comes with high robustness at the cost of higher computation time. The pixel size of the input image was set to be 640 $\times$ 640.

3.1 Zebrafish embryo detection results

The training results are summarized in the Table 3. The values of Precision, Recall and mAP are obtained using the equations respectively 3, 4, 6 The confusion matrix

Table 3 Training results for each class.

Classes	Precision	Recall	$mAP@0.5$	$mAP@0.5:0.95$
stage 1	0.732	0.814	0.851	0.732
stage 2	0.717	0.844	0.866	0.767
dead	0.894	0.905	0.95	0.772
advanced	0.902	0.838	0.941	0.801
returned	0.892	0.875	0.92	0.819
empty	0.865	83	0.921	0.798
holder	0.983	1	0.995	0.853
all	0.868	0.882	0.93	0.784

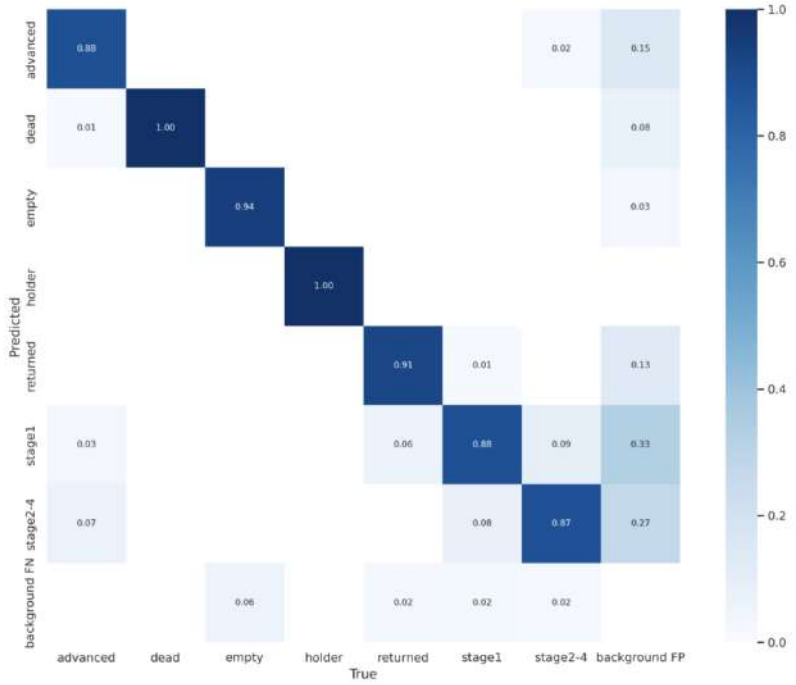

Fig. 6 Confusion matrix was made at IoU threshold of 0.45, confidence threshold of 0.25.

(see Fig.6) helps in understanding the classes that are being confused to other class. The *'empty'* and *'holder'* classes are the most precise and are not confused by any other class because simply they aren't look like them. Similarly *'dead'* class is not confused because, egg becomes degraded with whitish or black colors depending on

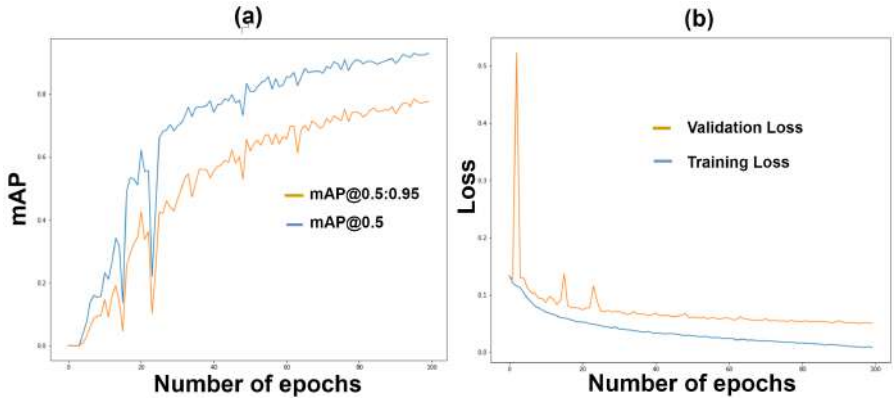

Fig. 7 Performance of first training. (a) $mAP@0.5$ and $mAP@0.5:0.95$ evolution through generations. (b) overall training loss and validation loss plotted using equation 2

the luminosity applied, this shows why they are not confused. The training loss serves as a measure to evaluate how well a deep learning model aligns with the training data. It gauges the model's error on the training set by reflecting how well the model is fitting the training dataset. It should decrease over time as the model learns from the dataset which is our case (see Fig.7). However, a very low training loss doesn't necessarily mean the model will perform well on new, unseen data, as it may have overfit the training data. Hence the usefulness of the validation loss which helps assess how well the model generalizes to data it hasn't seen during training. The two curves converge but with a shift all the same, which shows that the model learns well from training data but does not perform very well on validation data. So, the first training gives an accuracy of 0.93 but in order to have better results, we try to optimize the hyperparameters. *

Table 4 Optimized model results through generations

Generations	Precision	Recall	$mAP@0.5$	$mAP@0.5:0.95$
1	0.86711	0.9253	0.93	0.7884
2	0.8394	0.93655	0.93317	0.797
3	0.8671	0.8988	0.94145	0.8116
4	0.85584	0.9026	0.9374	0.80353
5	0.8425	0.9088	0.9231	0.7725
6	0.8619	0.9273	0.9459	0.8108
7	0.85676	0.93631	0.9428	0.8088
8	0.8668	0.9512	0.9480	0.8042
9	0.8858	0.8834	0.9392	0.7960
10	0.9015	0.9102	0.9545	0.8206

The optimization of the YOLOv5 model offers several advantages. As shown in Fig.9 and summarized in the Table 4, the model consistently achieves higher accuracy over generations. Therefore, the training and validation loss for the optimized YOLOv5 demonstrates a significantly better fit for the training and validation datasets. Unlike

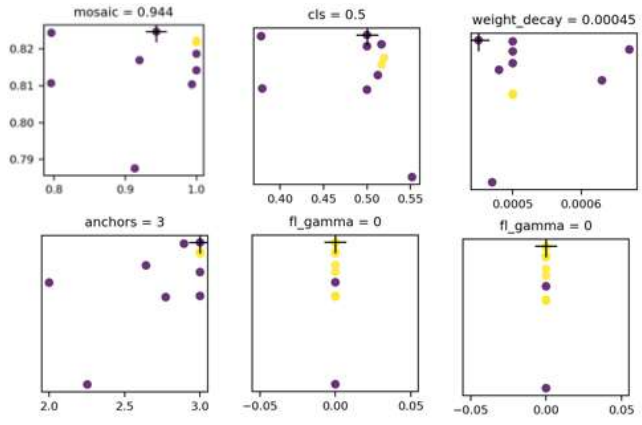

Fig. 8 Some hyperparameters tuning.Fitness score plotted on the y-axis and hyperparameter values on the x-axis, where greater concentrations are highlighted in yellow

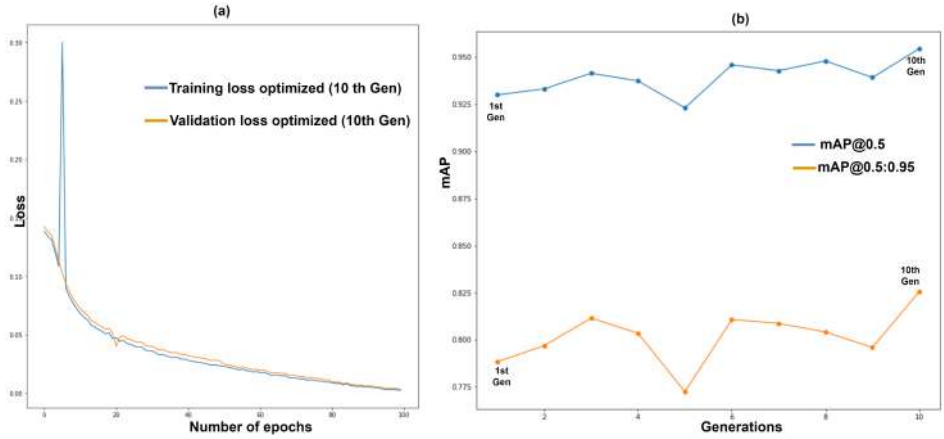

Fig. 9 (a) Overall training loss and validation loss optmized (10th generation) plotted using equation 2. (b) mAP@0.5 and mAP@0.5 : 0.95 evolution through generations

the default model, this one shows a loss validation curve which follows the loss training towards the end of the epoch. Our model provides accuracy of approximately 82% mAP@0.5:0.95 and 95.4% mAP@0.5, while the default model provides accuracy of approximately 78% mAP@0.5:0.95 and 93% mAP@0.5 after 100 epochs. Which is an increase of 4% and 2.4% respectively.

The model was tested on a testing database of 241 images. Using the same GPU , we obtained an accuracy of 95% with a detection speed of 10.6 ms per frame. The Figure 10 shows some examples of zebrafish egg detected with our trained model. The model is able to detect different stage of development of zebrafish egg as well as mortality with confidences above 90%.

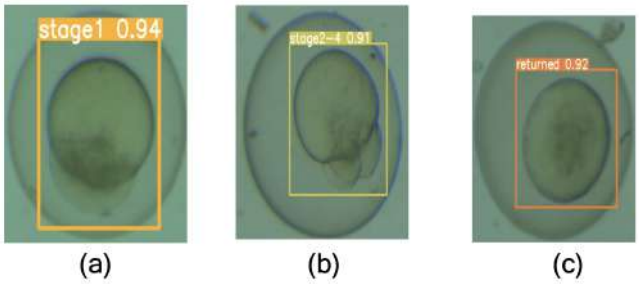

Fig. 10 Some examples of images coming from the test dataset with eggs detected by our model. (a) : stage 1 , (b) : stage 2-4 , (c) : returned

3.2 Zebrafish embryo sorting experiment result

The model optimized is used to perform zebrafish egg sorting. The experiment was carried out with 40 eggs for each trial separated into 20 dead eggs and 20 livable eggs at different stages of development. The eggs are injected with a pipette into the microfluidic chip at 1 hpf. After immobilization , the chip is placed in the XYZ-stage, then the sorting process begins. Six trials was performed, the first two trials without feedback use of dead egg position and the others with feedback use of dead egg position.

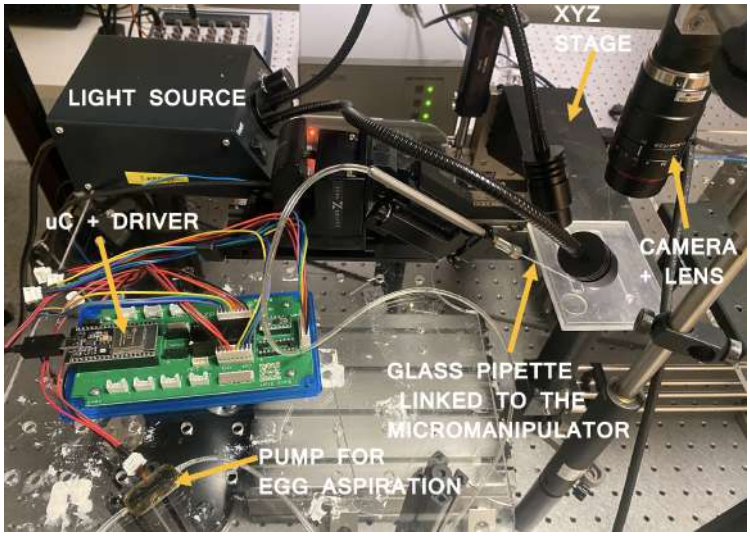

Fig. 11 Overview of the real system for the experiments.

3.2.1 Without feedback use of dead egg position

In this mode the XYZ-stage speed is set at 20mm/s and the manipulator at 4mm/s. The microfluidic chip is designed so that the traps all have the same horizontal distance

between them. The camera is being fixed and focus on a starting trap. The XYZ-stage is controlled in step by step mode. Each step of the XYZ-stage corresponds to a displacement from trap to trap and a focus of the camera on the following trap. The position of the traps being predefined, the micromanipulator is initialized by fixing Z and Y coordinates during the two first trials so that the holdertip glass faces the initial trap. We measure the necessary displacement along X from the initial position to reach the egg in the trap. This predefined distance is integrated into the coding program for access to an embryo in case of sorting. The first trial showed a major efficiency (100%) in the detection of eggs because all dead eggs and livable eggs were well detected, however, the pick and place procedure had a very low efficiency since only 5 of them was well picked. This was indeed due to a large part of the water in the system is removed by the pump system in the traps filling process to prevent zebrafish embryos displacement after immobilization. To overcome this, the pump was set in bidirectional mode. This allows to inject a quantity of water necessary for suction and then automatically suck the egg with this water injected in the trap. A second trial begins with a pump set to bidirectional mode for the suction process and results in a pick and place success percentage that has improved significantly from 20% of the first trial to 90%.

3.2.2 With feedback use of dead egg position

The previous trial gave satisfactory results. Nevertheless, the micro-displacements of the chip finally result from a bad position of the trap in the picking process but can be solved by fixing the chip on the XYZ-stage. Anyway, the first approach is weak in terms of adaptation because a small displacement of the chip or a change of position of the traps in the chip would limit the sorting process. We aim to make the holding pipette able to access to an egg according to the pixel coordinates of the egg. Given that the field of view (FoV) doesn't change during all the process because the camera is fixed, only two coordinates of the micromanipulator are used during the picking process namely X and Y. The displacement of the micromanipulator for the picking process is in reality only two translational movements, under the x and y axes, while z axis is fixed for all the process. We create an equation to map camera pixel Y*, X* coordinates of the holdertip to global reference frame X, Y coordinates of the micromanipulator. To do so, we choose an initial position of the holdertip in the FoV and make travel the micromanipulator along the y axis throughout the FoV by taking images and recording the real positions of the manipulator corresponding to each image. We do the same operation for the x axis. These images are then applied to our YOLO model detection algorithm by adding a segmentaion algorithm named YOLOv5 Instance Segmentation for the holding pipette which will allow to recover the pixel coordinates of the holdertip (see Fig.13(B)). We then plot the curves of the coordinates of the micromanipulator X , Y as a function of the pixel coordinates X* , Y* of the holdertip. The trend curves are thus recovered (see Fig.12). We obtain a relation between the variation of the pixel coordinates of the holdertip and global frame coordinates of the micromanipulator. Let's assume that the micromanipulator is at the initial position (Xi,Yi) global reference frame and the holdertip is at (X*,Y*) pixel coordinate (see Fig.13(A)). When a dead egg is detected by our model at (Xc,Yc)

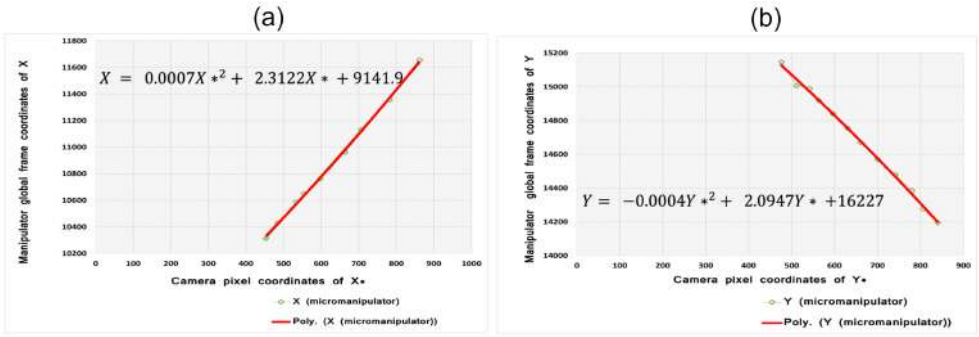

Fig. 12 (a): Manipulator global frame coordinates X in micrometer evolution in the FoV according to the holdertip pixel coordinates X*. (b): Manipulator global frame coordinates Y in micrometer evolution in the FoV according to the holdertip pixel coordinates Y*

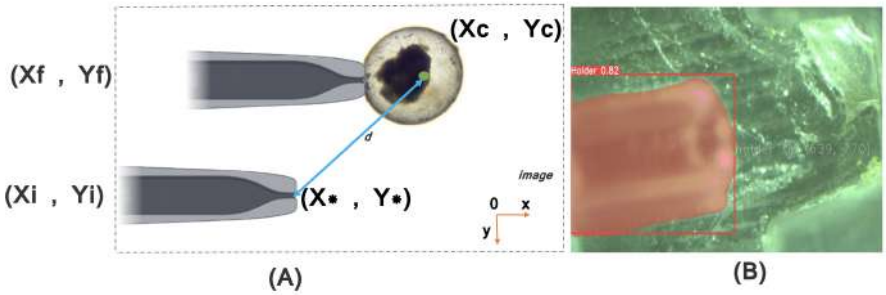

Fig. 13 Illustration of pipette displacement. (Xf,Yf) : Micromanipulator real frame coordinates (final position); (Xi,Yi) : Micromanipulator real frame coordinates (initial position); (X*,Y*) : Pixel coordinates of the holdertip ; (Xc,Yc) : Pixel coordinates of the cell. (B) An example of detection followed by segmentation of the holding pipette

pixel coordinates, to minimize the distance d between the holdertip and the dead egg, it suffices to calculate the global reference frame coordinates of the manipulator defined by the mapping equations:

$$Xf = 0.0007Xc^2 + 2.3122Xc + 9141.9 \tag{7}$$

$$Yf = -0.0004Yc^2 + 2.0947Yc + 16227 \tag{8}$$

With the equations thus obtained, it is possible to move the holdertip in the FoV based on the pixel coordinates of the egg and tests show a margin of error of $\pm 2\mu m$, which is acceptable considering the size of zebrafish embryo (0.7 mm). During trial 3, we define the initial position of the micromanipulator the same as when establishing the mapping. In this experiment, we move the stage continuously rather than in steps, and it only stops when a dead egg is found by the DL model. Dead eggs are reached by the glass pipette holder by putting the pixel coordinates of the detected cell into the equation (See equations 7 and 8). The two equations serve as a mapping tool that enables the holdertip to precisely locate and access dead eggs. In trials 3,4,5 and 6,

the implementation of these formulas resulted in a 97% success rate for the pick and place process but a decrease of the embryo's detection accuracy which is 98%. This decrease in the accuracy of the classification of zebrafish embryos may be due to the movement of the stage which is not adequate with the number of frames that the camera can take because certain embryos will require more stability to be well seen. For example, the camera can capture frames with images of half-viewed embryos. By further reducing the speed of the XYZ stage, we will be able to obtain better results at the expense of the speed of the sorting process.

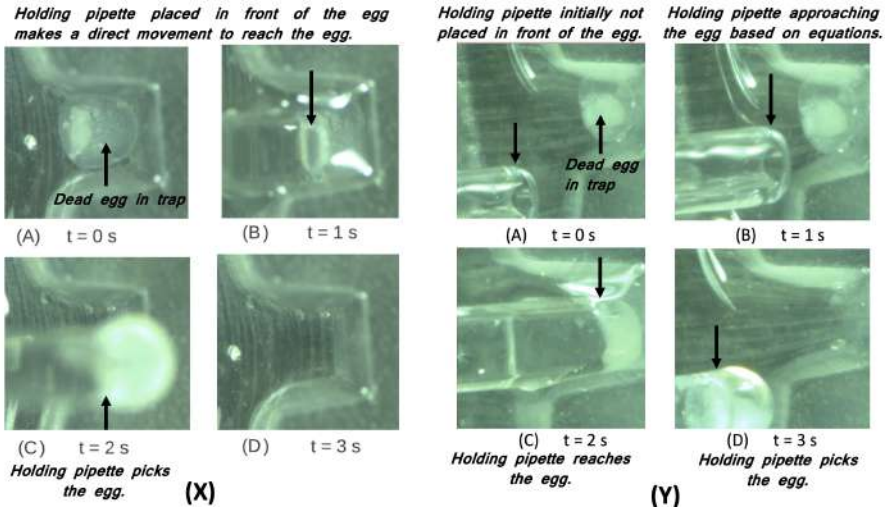

Fig. 14 X: Without feedback use of dead egg position. (X.A): Dead egg in the trap, , holdertip no need to be in the FoV. (X.B): access of the pipette in the trap, aspiration in progress with 500ml/min during 1 s. (X.C): Egg already picked. (X.D): Empty trap, after aspiration. Y: With feedback use of dead egg position. (Y.A): Dead egg in the trap, holdertip in the FoV. (Y.B): Holdertip going to the egg position using map equations. (Y.C): Aspiration in progress with 500ml/min during 1 s. (Y.D): Egg already picked, empty trap after aspiration. When using feedback of dead egg position, the holdertip can be anywhere in the FoV and manages to access the egg compared to the other mode , the holdertip must be initialized to be in front of the starting trap and only moves along x axis to acess the dead egg.

Sorting out dead or unfertilized zebrafish eggs is an important task for biologists. Our optimised detection model succeeds in detecting zebrafish eggs observed during the tests with acceptable accuracies which vary depending on the operating mode. Moreover, this is done with high processing speed (10.6 ms per frame), which makes it possible to fully explore the chip (36 egg traps) in 44 s if traps contain livable eggs or empty. The idea of the microfluidic chip greatly improves the pick and place or access to an egg in general, because it greatly reduces computation time while immobilizing the egg at the same time. The microfluidic chip allows eggs to be stored in cavities without handling them with contact, which can damage them. Without feedback use of dead egg position mode, the micromanipulator is calibrated so that the y and z axes are fixed. Knowing the distance between the cavities, the displacement of the

XYZ-stage is chosen as being the distance which separates the cavities. Therefore, the cavity must be in front of the pipette holding and a translation on the x axis will allow the embryo to be recovered as shown in figure 14(X.B). However, a simple calibration error will upset the process without use of feedback for the dead embryo position. Using a feedback mode ie with feedback use of dead egg position, gives us more efficiency in the picking process but decrease the scanning speed of the chip. In continuous mode, the experiments made have shown that the maximum speed of the XYZ-stage which allows detection of zebrafish eggs is around 4 mm/s. Under these conditions, our microfluidic chip is fully explored in around 52 s if all of the traps are empty or contain livable eggs. The feedback mode offers more robustness because, a change of the microfluidic chip and its characteristics or a micro-displacement of the chip will not affect the process. The holding pipette no longer needs to be exactly in front of the face of the embryo to access it. In figure **??**, the holding attacks the cell from the side and manages to find the cell using the equations and pixel coordinates of the center of the embryo. This is a major advantage of the feedback mode because the accuracy of sorting increases but the speed of the exploration of the chip is reduced. This is normal because closed-loop systems work precisely due to the feedback system. Open loop system usually gives fast response, while closed loop system gives slow response. A better approach which would combine the two advantages of the two modes would be to combine a movement of the XYZ stage in step by step mode with a high speed (20 mm/s) and use the map equations to find the embryos to be sorted. To demonsrate the superior side of our proposed automated zebrafish embryo sorting system, a comparison with similar works in the literature was conducted.

Table 5 Comparison of our work with the literature.

Tasks	Our work	[9]	[8]
Num. of eggs for sorting experiments	240	4752	694
Egg sorting accuracy	20% (trial 1) 90% (trial 2) 97.9% (trial 3,4,5 and 6 combined)	-	96.8%
Egg detection speed (per 1 egg)	10.6 ms	1 s	-
Egg sorting speed (per 1 egg)	3 s	14 s	8 s

Our sorting system (see Table 5) provides higher accuracy, egg detection and sorting speed compared to [8, 9]. However they have experimented with a larger number of zebrafish than ours. It is clear that nowadays the detection models are effective, the competition lies in the speed of execution of the task. Our work based on an optimized YOLOv5 model offers a much higher speed compared to the methods used in these two works, it is 94x faster than [9] based on template matching. Same observation for the speed of sorting an egg. In addition to the good immobilization and the sorting offered by the chip, it is believed that our approach may be useful in particular for rapid cell microinjection.

4 Conclusion

Using the deep learning detection algorithm YOLOv5, we have successfully developed a sorting system for identifying dead or unfertilized zebrafish eggs. After successful training, we were able to optimized the model to operate at a speed of 10.6 ms per frame with a 95% accuracy. This model was used for a sorting system composed of a microfluidic chip where the eggs are housed in cell traps, an XYZ-stage and a micromanipulator with a glass pipette as end-effector. Experiments finally showed a sorting efficiency of 97.9% for the feedback mode which is better than similar works. Future works will focus on cell sorting with DL and microfluidic chip without external element like micromanipulator or XYZ-stage, but only using water and pumping system to have a portable system.

Acknowledgements. The authors thank AbdelKarim Mannioui, PhD, Responsible for the Animal Facility and Engineering Aquatic Models Platform of Sorbonne University and Prof. Zizioli, researcher at Department of Molecular and Translational Medicine of Universita degli Studi di Brescia, as well as their team for providing us fresh zebrafish eggs

Declarartions

Funding

This study was funded by the Franco-Italian University (Université franco-italienne (UFI) / Università Italo Francese (UIF)).

Competing interest

The authors declare that they have no conflict of interest.

Ethics approval and consent to participate

Consent for publication

Data availability

The datasets supporting in this study are available from the corresponding author upon reasonable request.

Code availability

The codes used for zebrafish embryo detection and sorting in this study are publicly available at the GitHub repository: https://github.com/AliouneDiouf/zebappdetect.git

Author contribution

All authors have made substantial contributions regarding the conception and design of the study. Acquisition of images and analysis (AD, SH), development of the deep

learning model(AD, FS), Robotic phase sorting(AD, EG, MB), mechanical design and manufacturing of the microfluidic chip (AD, IF, GL) and final approval of the version submitted (all authors).

References

[1] Mohand Ousaid, A., Haliyo, S., Régnier, S., Hayward, V.: High fidelity force feedback facilitates manual injection in biological samples. IEEE Robotics and Automation Letters **5**(2), 1758–1763 (2020) https://doi.org/10.1109/LRA.2020.2969940

[2] Woynarovich, E., Horváth, L., *et al.*: The Artificial Propagation of Warm-water Finfishes: a Manual for Extension. vol. 201, (1980)

[3] Meyers, J.R.: Zebrafish: development of a vertebrate model organism. Current Protocols Essential Laboratory Techniques **16**(1), 19 (2018)

[4] Otterstrom, J.J., Lubin, A., Payne, E., Paran, Y.: Technologies bringing young zebrafish from a niche field to the limelight. SLAS technology (2022)

[5] LaBelle, C.A., Massaro, A., Cortés-Llanos, B., Sims, C.E., Allbritton, N.L.: Image-based live cell sorting. Trends in Biotechnology **39**(6), 613–623 (2021)

[6] Sadak, F., Saadat, M., Hajıyavand, A.M.: A vision-guided methodology for the automation of biological cell injection. In: 2020 2nd International Conference on Electrical, Control and Instrumentation Engineering (ICECIE), pp. 1–9 (2020). IEEE

[7] Schutera, M., Dickmeis, T., Mione, M., Peravali, R., Marcato, D., Reischl, M., Mikut, R., Pylatiuk, C.: Automated phenotype pattern recognition of zebrafish for high-throughput screening. Bioengineered **7**(4), 261–265 (2016)

[8] Graf, S.F.: Automated microinjection with integrated cell sorting, immobilization and collection. PhD thesis, ETH Zurich (2011)

[9] Breitwieser, H., Dickmeis, T., Vogt, M., Ferg, M., Pylatiuk, C.: Fully automated pipetting sorting system for different morphological phenotypes of zebrafish embryos. SLAS TECHNOLOGY: Translating Life Sciences Innovation **23**(2), 128–133 (2018)

[10] Shang, S., Long, L., Lin, S., Cong, F.: Automatic zebrafish egg phenotype recognition from bright-field microscopic images using deep convolutional neural network. Applied Sciences **9**(16), 3362 (2019)

[11] Ishaq, O., Sadanandan, S.K., Wählby, C.: Deep fish: deep learning–based classification of zebrafish deformation for high-throughput screening. SLAS Discovery: Advancing Life Sciences R&D **22**(1), 102–107 (2017)

[12] Čapek, D., Safroshkin, M., Morales-Navarrete, H., Toulany, N., Arutyunov, G., Kurzbach, A., Bihler, J., Hagauer, J., Kick, S., Jones, F., et al.: Embryonet: using deep learning to link embryonic phenotypes to signaling pathways. Nature Methods, 1–9 (2023)

[13] Cordero-Maldonado, M.L., Perathoner, S., Kolk, K.-J., Boland, R., Heins-Marroquin, U., Spaink, H.P., Meijer, A.H., Crawford, A.D., Sonneville, J.: Deep learning image recognition enables efficient genome editing in zebrafish by automated injections. PLoS One **14**(1), 0202377 (2019)

[14] Jones, R.A., Renshaw, M.J., Barry, D.J., Smith, J.C.: Automated staging of zebrafish embryos using machine learning. Wellcome Open Research **7**(275), 275 (2023)

[15] Zhu, F., Akagi, J., Hall, C.J., Crosier, K.E., Crosier, P.S., Delaage, P., Wlodkowic, D.: A high-throughput lab-on-a-chip interface for zebrafish embryo tests in drug discovery and ecotoxicology. In: Micro/Nano Materials, Devices, and Systems, vol. 8923, p. 892345 (2013). International Society for Optics and Photonics

[16] Lefevre, A., Gauthier, V., Gauthier, M., Bolopion, A.: Closed-Loop Control of Particles Based on Dielectrophoretic Actuation. IEEE/ASME Transactions on Mechatronics **1**, 1–10 (2022)

[17] Choudhury, D., Noort, D., Iliescu, C., Zheng, B., Poon, K.-L., Korzh, S., Korzh, V., Yu, H.: Fish and chips: a microfluidic perfusion platform for monitoring zebrafish development. Lab on a Chip **12**(5), 892–900 (2012)

[18] Li, Y., Yang, F., Chen, Z., Shi, L., Zhang, B., Pan, J., Li, X., Sun, D., Yang, H.: Zebrafish on a chip: a novel platform for real-time monitoring of drug-induced developmental toxicity. PLoS One **9**(4), 94792 (2014)

[19] Tang, X., Liu, X., Li, P., Liu, F., Kojima, M., Huang, Q., Arai, T.: On-chip cell–cell interaction monitoring at single-cell level by efficient immobilization of multiple cells in adjustable quantities. Analytical Chemistry **92**(17), 11607–11616 (2020)

[20] Chen, Z., Liu, X., Tang, X., Li, Y., Liu, D., Li, Y., Huang, Q., Arai, T.: On-chip automatic trapping and rotating for zebrafish embryo injection. IEEE Robotics and Automation Letters **7**(4), 10850–10856 (2022)

[21] Jocher, G.: ultralytics/yolov5: V3.1 - Bug Fixes and Performance Improvements. https://doi.org/10.5281/zenodo.4154370 . https://doi.org/10.5281/zenodo.4154370